Nuclear Magnetic Resonance Investigation of the Base-Pairing Structure of *Escherichia coli* $tRNA^{Tyr}$ Monomer and Dimer Conformations†

B. F. Rordorf‡ and D. R. Kearns*

ABSTRACT: The structures of the *Escherichia coli* tyrosine tRNA monomer and dimer have been investigated by high-resolution nuclear magnetic resonance (NMR). At 23 °C the monomer contains 26 ± 2 base pairs and the low-field NMR spectrum (11.7–15 ppm) can be accounted for in terms of the cloverleaf structure (23 base pairs) and three additional resonances that are assigned to tertiary structure base pairs. Assignments suggested for the various resonances are consistent with thermal denaturation studies in low-salt solutions. Under these conditions the temperature dependence of the spectrum can be interpreted in terms of sequential unfolding of the cloverleaf structure with the minor and dihydrouridine stems melting first, followed by the TψC stem, the anticodon stem, and finally the amino acceptor stem. Certain features of the tertiary structure of $tRNA^{Tyr}$ are similar to other tRNA, but some details of the folding must be different, since no resonance from the s^4U_8·A_{14} tertiary base pair is observed. The $tRNA^{Tyr}$ dimer contains only 20 ± 2 base pairs per tRNA (40/dimer) at 23 °C and a good account of the low-field NMR spectrum can be given in terms of a secondary structure in which bases of the TψC stem and loop are involved in intermolecular base pairing. Formation of the dimer requires opening of the hU and TψC stems, but not the anticodon or amino acid acceptor stems, and this fits well with relative stabilities observed for these stems in the monomer. The model also provides an explanation for the formation of $2n$-mers, that were stable enough to be separated by gel electrophoresis at room temperature (10 mM Mg^{2+}). Experimental conditions required for interconversion of monomer and dimer are also described.

Studies of the interaction between RNA molecules are of interest in a number of different contexts, including tRNA binding to ribosomes (Erdmann et al., 1973; Grummt et al., 1974; Richter et al., 1974), intermolecular association of different (Eisinger and Gross, 1974) and identical tRNA (Loehr and Keller, 1968; Zachau, 1968; Yang et al., 1972; Söll et al., 1967; Kowalski and Fresco, 1971) in solution, the interaction of tRNA with small oligonucleotides (Uhlenbeck, 1972; Schimmel et al., 1972; Pongs et al., 1971; Eisinger and Spahr, 1973; Högenaur, 1970), and the formation of stable or metastable denatured conformations of tRNA (Adams et al., 1967; Streeck and Zachau, 1972; Kearns et al., 1974; Hawkins and Chang, 1974). As pointed out by Yang et al. (1972), the dimerization of certain tRNAs provides a useful model system for studying RNA–RNA interactions, and there have been several previous studies of the self-dimerization of tRNA. The most extensive work concerns the dimerization of *Escherichia coli* $tRNA^{Tyr}$ where thermodynamic, kinetic, and spectroscopic measurements of the monomer to dimer conversion were carried out. On the basis of these data Yang et al. (1972) proposed a model for the secondary structure of the dimer, but at that time no reliable method had been developed for counting base pairs and distinguishing between alternative base-pairing schemes.

Through the application of high-resolution NMR it is now possible to obtain a great deal of information regarding the structure of tRNA molecules in solution (Kearns and Shulman, 1974). From an integration of the low-field NMR spectra the total number of base pairs (secondary and tertiary structure) can be determined, and an estimate of the approximate numbers of A·U and G·C base pairs can be obtained. By application of a semiempirical ring current shift theory (Kearns and Shulman, 1974) the spectra of different possible secondary structures can be computed and compared with the observed spectra, and in this way the most plausible structures can be identified. Finally, from the temperature dependence of the NMR spectra, some specific assignments can be tested. In the present paper we have used NMR to investigate the base pairing structure of *E. coli* $tRNA^{Tyr}$ monomers and dimers. We first show that the spectrum of the monomer can be accounted for in terms of the cloverleaf structure and three additional tertiary structure base pairs. The spectral changes that occur upon converting the monomer to the dimer are then used, in conjunction with other NMR data, to develop a plausible structure for the dimer.

Materials and Methods

tRNA Samples. Tyrosine-accepting tRNA from *E. coli* (a mixture of $tRNA^{Tyr}_I$ + $tRNA^{Tyr}_{II}$) was prepared from crude *E. coli* tRNA by Dr. Brian R. Reid, University of California, Riverside. The tyrosine accepting tRNA was purified from the 10% ethanol elute of a BD-cellulose column (Gillam et al., 1967), first by a DEAE-Sephadex A-50 with a linear salt gradient (Nishimura et al., 1967), and then by BD-cellulose (2 × 90 cm) with a linear gradient 21 each of 0.8 and 1.2 M NaCl, 10% ethanol (50 mM NaOAc, 10 mM $MgCl_2$, pH 5.0). The final mixture of $tRNA^{Tyr}_I$ and $tRNA^{Tyr}_{II}$ accepted 1590 pmol of tyrosine per A_{260} of $tRNA^{Tyr}$. The absorbance at the 335-nm 4-thiouridine peak was found to be 4% of the 260-nm

† From the Department of Chemistry, University of California, Riverside, California 92502. *Received July 28, 1975.* Supported by grants from the United States Public Health Service (GM 21431) and the National Science Foundation (GB-41110).

‡ Submitted in partial fulfillment of the requirements for the Ph.D. degree in Chemistry at the University of California, Riverside.

* Address correspondence to: Department of Chemistry, University of California, San Diego, La Jolla, Calif. 92037.

[1] Abbreviations used are: NMR, nuclear magnetic resonance; hU, dihydrouridine; DEAE, diethylaminoethyl; EDTA, (ethylenedinitrilo)-tetracetic acid.

[2] The subscript ~ refers to an average value.

absorbance. Some studies were also carried out on a sample of tRNA$^{Tyr}_{I}$ (greater than 90% pure) prepared by Mr. P. Bolton in our laboratory.

Gel Electrophoresis. The analytical separation of tRNA polymers was performed under nondissociating conditions (0.1 M NaCl, 10 mM $MgCl_2$, and 10 mM sodium cacodylate, pH 7.0) on running gels containing 10% (5%) acrylamide and 0.25% (0.125%) methylenebisacrylamide using currents of 12 mA/column and running times of typically 6 h. Gels were calibrated with tRNAs, 5S RNA, yeast tRNA^{Ala} polymers (reannealed at 40 mg/ml in the absence of magnesium), and with citrus exocortis viroid (mol wt ca. 100 000; Semancik et al., 1975). The preparation and analysis of the gels were described elsewhere (Rordorf and Kearns, 1976a).

Optical Melting Curves. The melting curves were obtained with a rapid heating/cooling device (Rordorf and Kearns, 1976b) in a sealed 1-mm path-length cuvette.

NMR Spectra. All NMR spectra were obtained with a Varian HR-300 spectrometer operated in field sweep mode, and a Nicolet 1020 signal averager computer was used to accumulate spectra for up to 3 h. Transfer RNA concentrations on the order of 4 mg/120 μl were used and temperatures were controlled to ±1 °C.

NMR samples of tRNA^{Tyr} monomers (30–40 mg/ml) in high-salt solutions (0.1 M NaCl) contained 1 mM $MgCl_2$ to prevent premature dimerization. Dimerizations were performed directly in the NMR tube (after removal of the Mg(II) by addition of EDTA to 2 mM) by slowly (2 h) cooling from 70 to 24 °C. Dimers were converted to monomers by slow reannealing from 70 °C under low-salt conditions (1 mM $Na_2S_2O_3$, dialyzed at pH 7.0) and were concentrated by vacuum dialysis at 4 °C. Gel electrophoresis was used to establish that samples referred to either as monomeric or dimeric tRNA^{Tyr} contained at least 90% monomer or dimer, respectively, before and after the NMR measurements. Cases in which there was partial interconversion between monomer and dimer are indicated.

Simulated spectra were calculated on a PDP-12 computer with the spectrum processing program CATACAL by adding up Lorentzian peaks of equal heights and half-width (18 Hz = 0.06 ppm for monomer, 24 Hz = 0.08 ppm for dimer). The relative intensity distribution, the spectral shape, and the correct location of the spectral maxima were used as criteria for the fit. The resonance positions determined by these computer analyses were subsequently used in the assignment of the low-field NMR spectra (Table II).

The semiempirical ring current shift theory used to predict the low-field NMR spectra of tRNA has been discussed extensively elsewhere (Kearns et al., 1974; Kearns and Shulman, 1974). The base pairing matrix used in the analysis is shown in Figure 1.

Results

Number of Exchangeable Protons in the Low-Field NMR Spectra of tRNA^{Tyr} Monomer. Determination of the number of exchangeable resonances in the low-field NMR spectrum (from 11.7 to 15 ppm) of the monomer and the dimer conformations of tRNA^{Tyr} is crucial to a proper interpretation of the spectra and to the development of a model for the dimer conformation. In previous studies the low-field spectra have been integrated by comparing the tRNA spectra with the spectrum of some "standard" such as metcyanomyoglobin (Kearns et al., 1971a,b), or by *assuming* that some well resolved resonance in the low-field spectrum corresponds to an integral number of protons (Lightfoot et al., 1973). Neither of these methods is particularly accurate and in the present work, we have compared the intensity in the low-field region of the spectrum (obtained in H_2O) with the intensity in the aromatic region of the spectrum (6.5–9 ppm) obtained in D_2O under identical operation conditions (rf power, sweep width, etc.). The conversion from H_2O to D_2O was carried out *directly* in the NMR tube by repeated (four times) concentration of the sample to one-fourth of its initial volume and dilution with aliquots of D_2O. In order to prove that spectra in D_2O and H_2O were directly comparable, the methyl resonances of the monomer (located around 1 and 1.2 ppm) were also monitored before and after the solvent change. Additional details regarding the integration of the low-field spectra of tRNA^{Tyr} and eight other tRNA are to be given elsewhere (Bolton et al., 1976).

The results of this comparison are shown in Figure 2 and Table I. Assuming there are 103 resonances in the aromatic region between 6.5 and 9 ppm (Goodman et al., 1968), we found 26 ± 2 exchangeable resonances in the low-field spectrum of the monomer between 11.7 and 15 ppm both in samples of pure tRNA$^{Tyr}_{I}$ and in the mixture of tRNA$^{Tyr}_{I,II}$.

The low-field spectrum of tRNA^{Tyr} monomer measured in solutions containing low salt (sample prepared by dialysis against 1 mM $Na_2S_2O_3$, pH 7.0, or by addition of 10 mM cacodylate buffer, pH 7.0, to salt free lyophylized sample) is rather different from that obtained under normal (0.1 M NaCl) salt conditions (Figure 3a,c). However, upon addition of magnesium to 10 mM Mg to this sample (Figure 3b) the spectrum originally obtained in high salt is regained. By directly comparing spectra before and after the addition of Mg(II), and by assuming that the latter spectrum contains 26 resonances, the low-salt spectrum is found to contain only 17 ± 2 resonances (Table I). A computer fit of the low-salt spectrum also is consistent with 17 resonances (see Figure 3c and Table II).

Thermal Unfolding of the tRNA^{Tyr} Monomer. In the high-salt solutions (0.1 M NaCl) there is little change in the low-field spectrum of the monomer between 20 and 40 °C, except at 13.8 ppm (assigned to a tertiary structure base pair) where a small loss of intensity occurs (Figure 4). Unfortunately, it was not possible to study the thermal denaturation of tRNA^{Tyr} monomer in this solution above 45 °C because of rapid formation of dimers (half-life for dimer formation ~13 ± 3 min at 50 °C; Rordorf, Thesis). The temperature dependence of the tRNA^{Tyr} monomer spectrum in low salt (1 mM $Na_2S_2O_3$) at pH 7 is shown for comparison in Figure 5.

Salt and Magnesium Dependence of the Monomer–Dimer Equilibrium of tRNA^{Tyr}. Gel electrophoresis was used to study the monomer–dimer equilibrium under a variety of experimental conditions, with the following results. A slow dimerization was observed at temperatures as low as 10 °C when monomeric tRNA^{Tyr} is dissolved in solutions containing 0.1 M NaCl but no magnesium (Figure 6a). The absence of magnesium was found to be important for a complete conversion to dimers even with the relatively high tRNA concentrations (up to ~40 mg/ml) used in our experiments (Figures 6b and 7d). Fast cooling under high salt (0.1 M NaCl), no magnesium conditions led to some trimer formation (Figure 7c), whereas slow cooling (from 70 °C) led to a more complete dimerization (Figure 7d) and aggregates involving even numbers of tRNA (20–25% 2n-mers with $n >$ 1: Figure 7e).

In the presence of magnesium fast cooling (from 70 °C) leads to more extensive dimerization than does slow reannealing (Figure 6bc), indicating that magnesium preferentially stabilizes the low-temperature monomer structure.

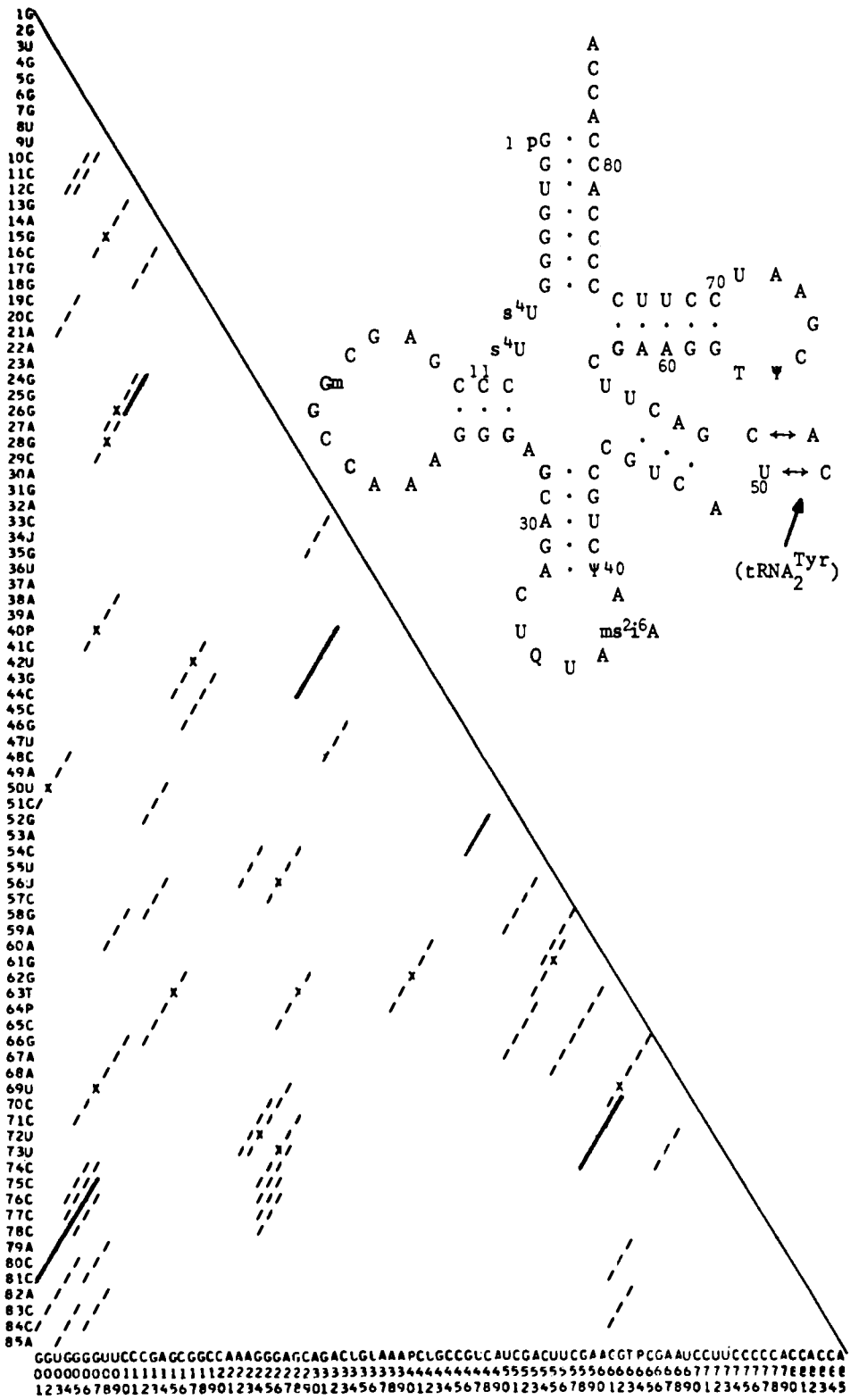

FIGURE 1: Base pairing matrix for *E. coli* $tRNA^{Tyr}_1$. AU, Aψ, and GC Watson–Crick base pairs (/), GU base pairs (X), and cloverleaf helices (–). The complete dimer base pairing matrix is obtained by reflection of the monomer matrix about its diagonal.

A completely different situation arises in *very* low-salt solutions (1 mM $Na_2S_2O_3$, dialyzed) where reannealing of highly concentrated samples (30 mg/ml) in magnesium-free solutions led to an almost complete return to monomers (Figure 6d). This is probably due to an incomplete neutralization of the phosphate backbone (some sodium dissociation resulting in an electrostatic repulsion of the individual tRNAs). Since the concentration of magnesium ion in cells is on the order of 5 mM (Williams, 1970) we would conclude that dimerization of the tyrosine molecules is not important under normal physiological conditions. If, for some reason, the magnesium concentration was substantially reduced, then dimerization might become a problem, particularly at elevated temperatures.

Number of Exchangeable Protons in the Low-Field NMR

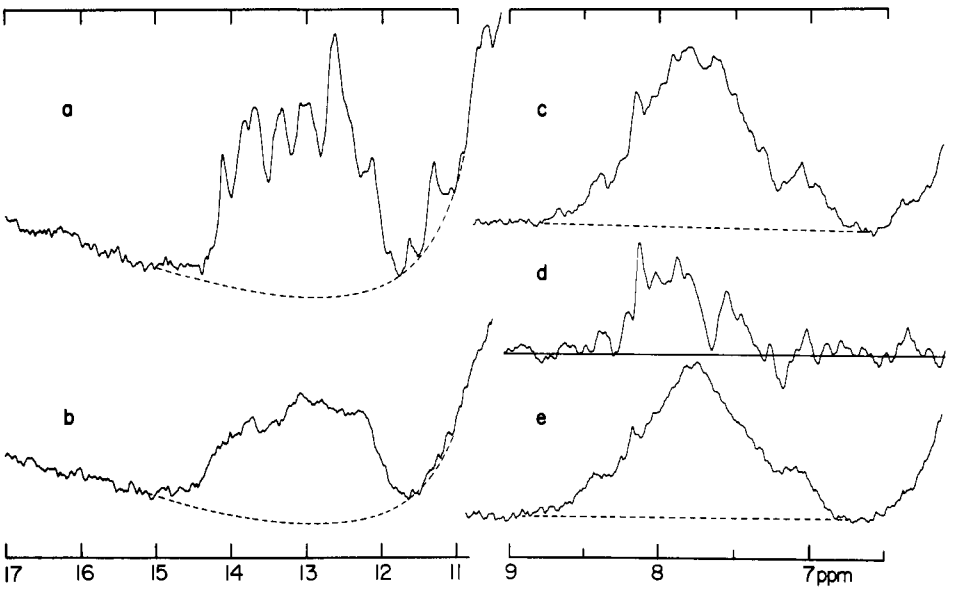

FIGURE 2: Direct intensity comparison of the high-resolution NMR spectra (23 °C) of *E. coli* tRNA^{Tyr} before and after dimerization in the NMR tube. The spectra shown include the low-field spectrum of monomer (a) and dimer (b) and aromatic spectrum in D_2O of monomer (c) and dimer (e) and difference spectrum (d) obtained by substracting spectrum e from c. The baselines assumed in the integrations are indicated by dashed lines. The solvent contained in 0.1 M NaCl, 10 mM cacodylic acid (pH 7.0), 1 mM $MgCl_2$, 2 mM EDTA, and 1 mM $Na_2S_2O_3$.

TABLE I: Intensity Comparisons between NMR Spectra of *E. coli* tRNA^{Tyr} in Its Monomer and Dimer Conformation.

Conformer	Spectral Region	Figure	Temp (°C)	Solvent	No. of Exchangeable Protons	
			Determination of Number of Exchangeable Protons in the Low-Field Region			
Monomer	Aromatic	2c	23	D_2O	103	
Monomer	Low field	2a	23	H_2O		26 ± 2
Monomer	Low field	3b	23	H_2O:10 mM Mg^{2+}	25-26	
Monomer	Low field	3c	23	H_2O:1 mM Na^+		18 ± 2
Monomer	Low field	5	45	H_2O	11	
Monomer[a]	Low field	5	33	H_2O		14
Monomer[a]	Low field	5	23	H_2O		17 ± 1
Dimer	Aromatic	8a	23	D_2O	103	
Dimer[b]	Low field	9	23	H_2O		21 ± 2
Dimer	Aromatic	8b	55	H_2O	103	
Dimer	Low field	9	55	H_2O		20 ± 2
Dimer	Low field	9	55	H_2O	19	
Dimer[a]	Low field	9	23	H_2O		21 ± 1
Monomer	Low field	2a	23	H_2O	26	
Dimer[c]	Low field	2b	23	H_2O		21 ± 2
					Intensity Assumed	Intensity Calcd
			Determination of Observable NMR Intensity at 23 °C after Dimerization			
Monomer	Aromatic	2c	23	D_2O	100	
Dimer[d]	Aromatic	2e	23	D_2O		82 ± 1
Dimer	Aromatic	8a	68	D_2O	100	
Dimer[a]	Aromatic	8a	23	D_2O		83 ± 2

[a] Temperature dependence of aromatic spectrum of yeast unfractionated tRNA was used for intensity calibration. [b] Relative tRNA concentration in H_2O vs. D_2O sample was determined by comparison of aromatic spectra at 68 °C. [c] Observable tRNA concentration was assumed to correspond to 82% of monomer concentration (from Table Ib: intensity comparison of aromatic spectrum before and after dimerization). [d] Acrylamide gel electrophoresis analysis of the dimerized NMR sample indicated the presence of 2.9% monomer, 73.8% dimer, 16.3% tetramer, 5.9% hexamer, and 1.1% octamer (23.3% $2n$-mer with $n > 1$).

Spectra of tRNA^{Tyr} Dimer. Two different methods were used to determine the number of base pairs present in the dimer at 32 °C. In the first method an NMR sample of monomer was dimerized in the NMR tube and the intensity in the low-field region and in the aromatic region of the spectrum were measured before and after the conversion to dimer (Figure 2; Table

TABLE II: Predicted and Observed Positions of the Resonances of the Low-Field NMR Spectra of *E. coli* $tRNA^{Tyr}$.[a]

Base Pair	Ring Current Shift Prediction	Computer Fit of the Low Field NMR Spectra of *E. coli* $tRNA^{Tyr}$ Monomer: High salt 34 °C (Figure 3a)	Monomer: 10 mM $MgCl_2$ 23 °C (Figure 3b)	Monomer: Low salt 23 °C (Figure 3b)	Monomer: Low salt 45 °C (Figure 5)	Dimer 32 °C (Figure 12a)	Dimer 55 °C (Figure 12b)
A_{68}·T_{63}	(14.4)					((1440))	
A_{60}·U_{72}	(13.8)	1400	1400	1403		1395	1380
A_{53}·U_{47}	(14.2)	1380	1380			1377	(1365)
Tertiary structure		1380	1380				
Tertiary structure		1375	1375				
A_{79}·U_3	(13.8)	1361	1363	1362	~1353	1363	1350
G_{46}·C_{54}	(13.4–13.5)	1361	1360			((1360))	
G_{62}·C_{70}	13.25–13.35)	1337	1336	1335		1353	1340
A_{30}·U_{42}	(13.3)	1330	1327	1332	1326	1342	1315
C_2·C_{80}	(13.25)	1325	1325	1330	~1315	1327	1310
A_{59}·U_{73}	(13.2)	1320	1320	1322		1308	1305
G_{28}·C_{44}	(13.15–13.40)	1303	1300	1308	1309	1299	1302
A_{32}·ψ_{40}	(13.2–13.3)	1300	1300	1300	—	1295	
Tertiary structure		1299					
G_7·C_{75}	(12.65–13.25)	1286	1295	1289	~1288	1286	1288
G_{61}·C_{71}	(12.8)	1282	1283	1267		1272	1283
G_6·C_{76}	(12.65)	1265	1272	1257	~1262	1266	1265
G_5·C_{77}	(12.65)	1260	1267	1251	~1250	1258	1260
G_{25}·C_{11}	(12.65)	1255	1257				
G_{24}·C_{12}	(12.5–12.9)	1255	1254				
G_{52}·C_{48}	(11.5–12.5)	1250	1250			((1250))	
G_{43}·C_{29}	(12.4)	1247	1246	1247	1245	1246	1245
G_{31}·C_{41}	(12.4)	1242	1233	1210	1210	1237	1230
G_{26}·C_{10}	(12.25–13.35)	1234	1228				
G_{58}·C_{74}	(12.25–12.50)	1217	1217	1205		1225	1220
A_{67}·ψ_{64}	(12.2)					1216	1215
G_1·C_{81}	(11.9–12.9)	1210	1205	1205	~1205	1208	1210
G_4·C_{78}	(11.9)	1208	1202	1195	~1200	1199	1205
G_{66}·C_{65}	(11.8)					1190	1190

[a] Only italicized resonances are present at 52 °C in the monomer spectrum under low-salt conditions. Single bracket: presence uncertain; double bracket: present only below 32 °C.

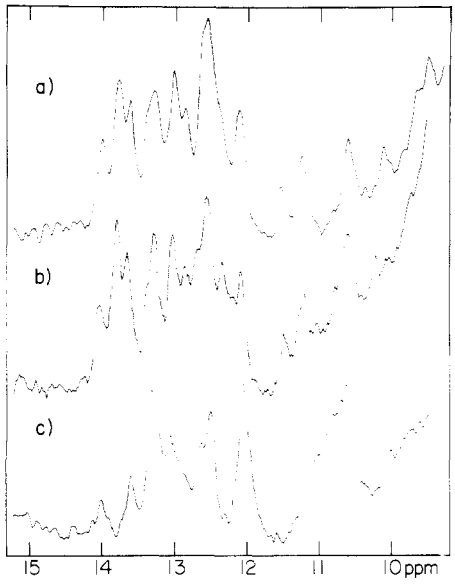

FIGURE 3: Comparison of the low-field NMR spectra (–) of *E. coli* $tRNA^{Tyr}$ (monomer) (a) in high salt (34 °C spectrum of Figure 4), (b) in 10 mM $MgCl_2$ (added), 1 mM $Na_2S_2O_3$ (dialyzed), and (c) in low salt (23 °C spectrum of Figure 5) with the computer simulated spectra (. . . . . .) that contains 26 (a), 25 (b), and 17 (c) Lorentzian peaks of equal height and half-width (18 Hz = 0.06 ppm) at positions summarized in Table II.

1). There is a substantial loss of intensity both in the low-field and aromatic regions (Figure 2) upon dimerization. The latter finding indicates that high-molecular-weight aggregates are formed (inhomogeneous line broadening) and necessitates a correction of the low-field intensity comparison for the polymerization effect. The formation of higher aggregates is supported by the temperature dependence of the aromatic spectrum of the dimer, where an *increase* of intensity (relative to a standard sample of unfractionated tRNA in D_2O) was observed upon raising the temperature (Figure 8 and Table I), and by direct observation of $2n$-mers by gel electrophoresis (Figure 7e).

Since monomer contains 26 base pairs, we find that the dimer contains only 20 ± 2 base pairs (Table I). In the second method, we compared the integrated intensity in the low-field region (measured in H_2O) with the intensity in the aromatic region of the spectrum (obtained in both D_2O and H_2O) and again obtained a value of 20 base pairs/tRNA, which is about 6 less that we found for the monomer (Figures 8, 9 and Table I).

Before proceeding further with the analysis it is important to consider the possibility that loss of resonances in the NMR spectrum upon dimer formation could be due to rapid opening and closing of certain helices of the dimer. This would broaden the resonances from the associated base pairs and could lead to an apparent loss of intensity in the NMR spectrum, although

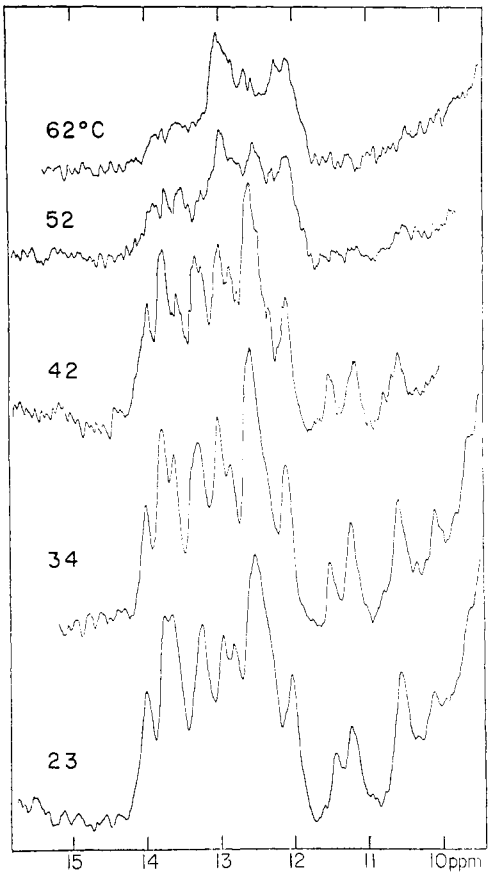

FIGURE 4: Temperature dependence of the low-field NMR spectrum of *E. coli* tRNA^{Tyr} (monomer) in 0.1 M NaCl, 10 mM cacodylic acid (pH 7.0), and 10 mM $MgCl_2$ (high salt).

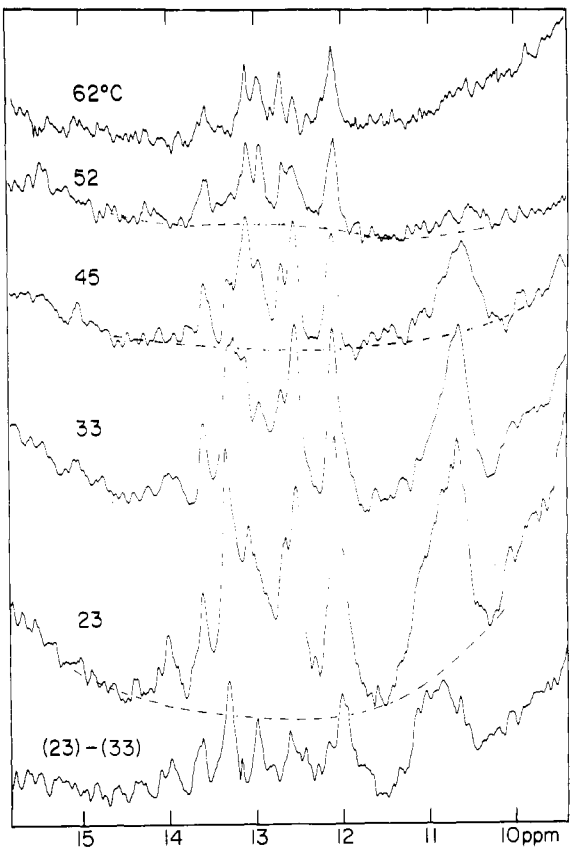

FIGURE 5: Temperature dependence of the low-field NMR spectrum of *E. coli* tRNA^{Tyr} (monomer) in 1 mM $Na_2S_2O_3$ (added by vacuum dialysis at pH 7.0) (low salt). Identical spectra were obtained in the presence of 10 mM cacodylic acid (pH 7.0). The difference spectrum obtained by subtraction of the 33 from the 23 °C spectrum is also shown at the bottom of the figure.

there was actually a gain in the total number (time average) of base pairs (Crothers et al., 1973). We believe this is not the explanation, since we have observed extra base pairs resulting from the dimerization of various fragments of tRNA (Rordorf and Kearns, 1975). Since, in these cases, the equilibrium constants for dimer formation are much smaller (melting point below 20 °C) than in the present case, we conclude that the observed loss of intensity in the NMR spectrum does correspond to a loss of 6 base pairs/molecule upon dimer formation. This loss of base pairs rules out most of the dimer structures that could have been expected from a consideration of the base pairing matrix (Figure 1). The temperature dependence of the dimer low-field NMR spectrum (19 resonances at 55 °C; Figure 9), on the other hand, points to a surprisingly high stability for the dimer structure.

Discussion

We now describe the way in which the NMR measurements and other results have been used to investigate the conformations of the monomeric and dimeric forms of *E. coli* tRNA^{Tyr}. In order to extract structural information from the low-field NMR spectra the following steps were carried out: (i) The low-field spectra were integrated to determine the total number of secondary and tertiary structure base per molecule, (ii) a computer fit of the spectra was obtained to determine the positions of individual resonances in the spectrum, and (iii) a semiempirical ring current shift theory (Kearns and Shulman, 1974) and base-pairing matrix (Figure 1) was used to examine various secondary and tertiary structures to find one(s) that could adequately account for the spectrum.

We first discuss the application of these procedures to the tRNA^{Tyr} monomer and show that the secondary structure can be well accounted for in terms of the cloverleaf model. The tertiary structure of this molecule appears, however, to be different from other Class I tRNA that we have examined. The changes in the NMR spectra (intensity and spectral distribution) that occur upon dimerization are then used along with other observations to develop a model for the secondary structure of the tRNA^{Tyr} dimer.

Assignment of the Low-Field NMR Spectra of tRNA^{Tyr} Monomer under High-Salt Conditions. tRNA$^{Tyr}_{I}$ and tRNA$^{Tyr}_{II}$ differ by only two nucleotides in the extra-arm loop (Figure 1), and, therefore, to a first approximation, both species should give identical low-field NMR spectra. This expectation was confirmed by a comparison of the low-field spectra of the mixture (30% tRNA$^{Tyr}_{II}$) with that of tRNA$^{Tyr}_{I}$ at 23 °C (H. Chao, unpublished results).

The number of exchangeable resonances (26 ± 2) in the monomer spectrum indicates that all stems of the cloverleaf structure are present in solutions containing 0.1 M NaCl, or 10 mM Mg(II), or both. To assign the low-field spectra, the ring current shift theory was used to calculate the resonance positions expected for a cloverleaf structure and these results are summarized in Table II. In general, there is good agreement between the computed and observed positions of resonances (standard deviation = 0.13 ppm). However, in the absence of additional data (e.g., thermal denaturation, chemical modification, etc.), we cannot be certain about the

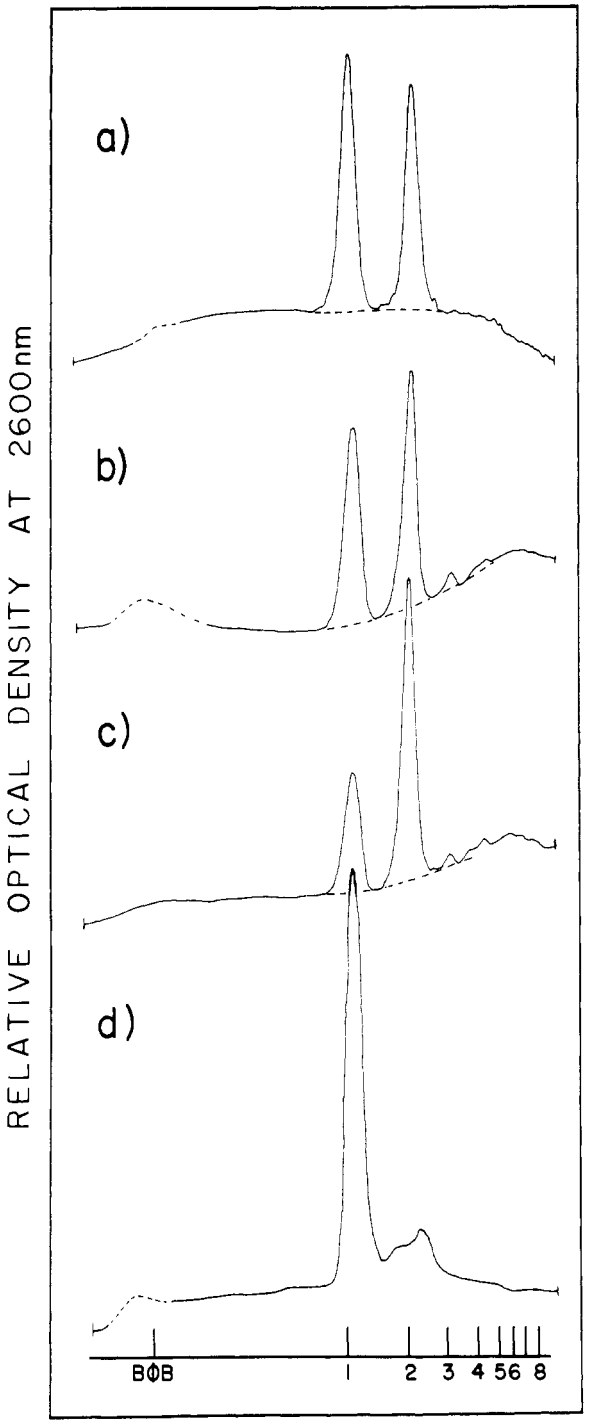

FIGURE 6: Effect of salt and magnesium on the monomer-dimer equilibrium of *E. coli* $tRNA^{Tyr}$. Gel electrophoresis analysis of (a) "monomer" sample (30 mg/ml) stored for 24 h in 0.1 M NaCl, 10 mM cacodylic acid (pH 7.0), and 10 mM EDTA (10 °C). (b) Dimerization by slow cooling (2 h), and (c) by trapping from 70 °C in the presence of 50 mM $MgCl_2$ (other conditions as in Figure 7c,d). (d) Monomerization by slow cooling (2 h from 70 °C in 1 mM $Na_2S_2O_3$ (added by vacuum dialysis at pH 7.0) at a tRNA concentration of 30 mg/ml (same sample as in Figure 5). The size of the *n*-mers is indicated at the bottom of the figure (from Figure 7a-d).

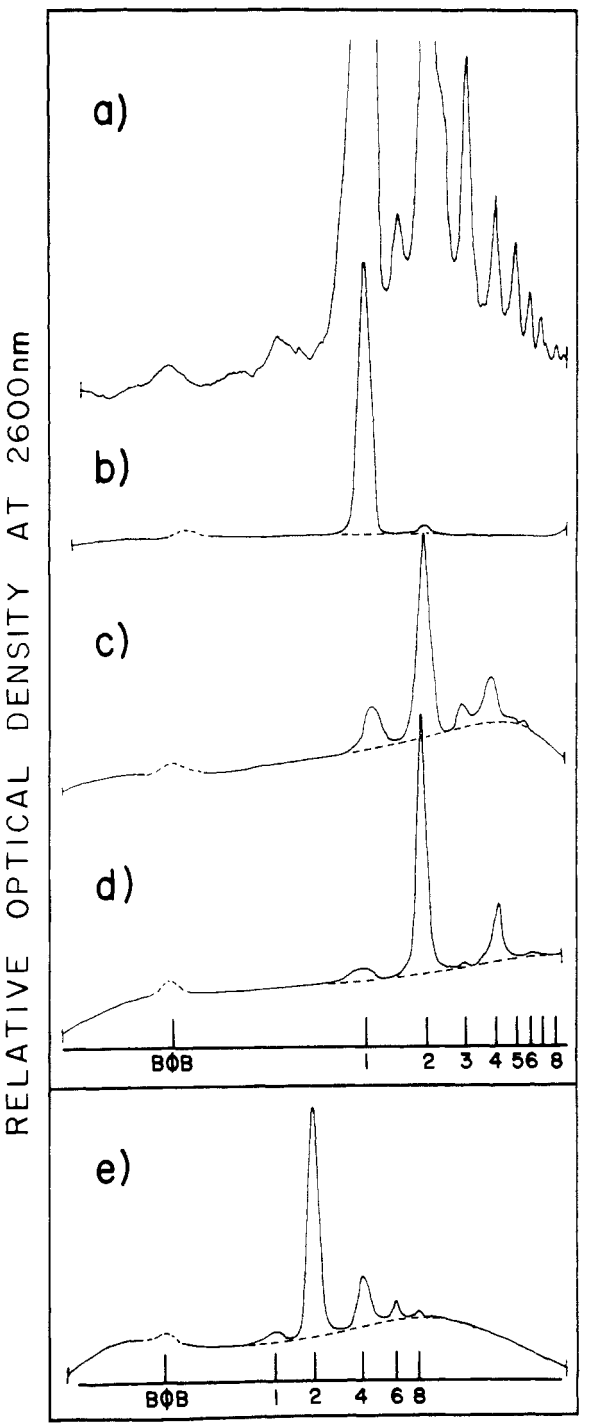

FIGURE 7: Gel electrophoresis analysis of $tRNA^{Tyr}$ aggregates. Polymerized yeast $tRNA^{Ala}$ is used for gel calibration (a). Gel analysis of NMR sample of Figure 2 before (b) and after dimerization by trapping from 70 °C (c) or by slow cooling (2 h) from 70 °C (d and e). Migration from right to left, size is given in units of tRNA (monomer), BΦB = bromophenol blue, acrylamide density is 10% (a-d) or 5% (e).

assignment of each individual resonance in the spectrum for several reasons. First of all, the ring current shift theory is only approximate (say within 0.1-0.2 ppm) because it does not explicitly include second nearest-neighbor effects. Secondly, the calculations are based on the assumption that all of the secondary structure helices are regular RNA helices. Finally, we know from studies of other tRNA (e.g., *E. coli* $tRNA^{Glu,Trp}$) that the positions of certain resonances are anomalous. These limitations must, therefore, be kept in mind as we discuss the interpretation of the results.

The cloverleaf secondary structure permits us to account for 23 of the 26 resonances observed in the low-field spectrum between 11.7 and 15 ppm. The three extra resonances (located at 13.8, 13.75, and 13.0 ppm, respectively) are assigned to tertiary structure base pairs for the following reason. We re-

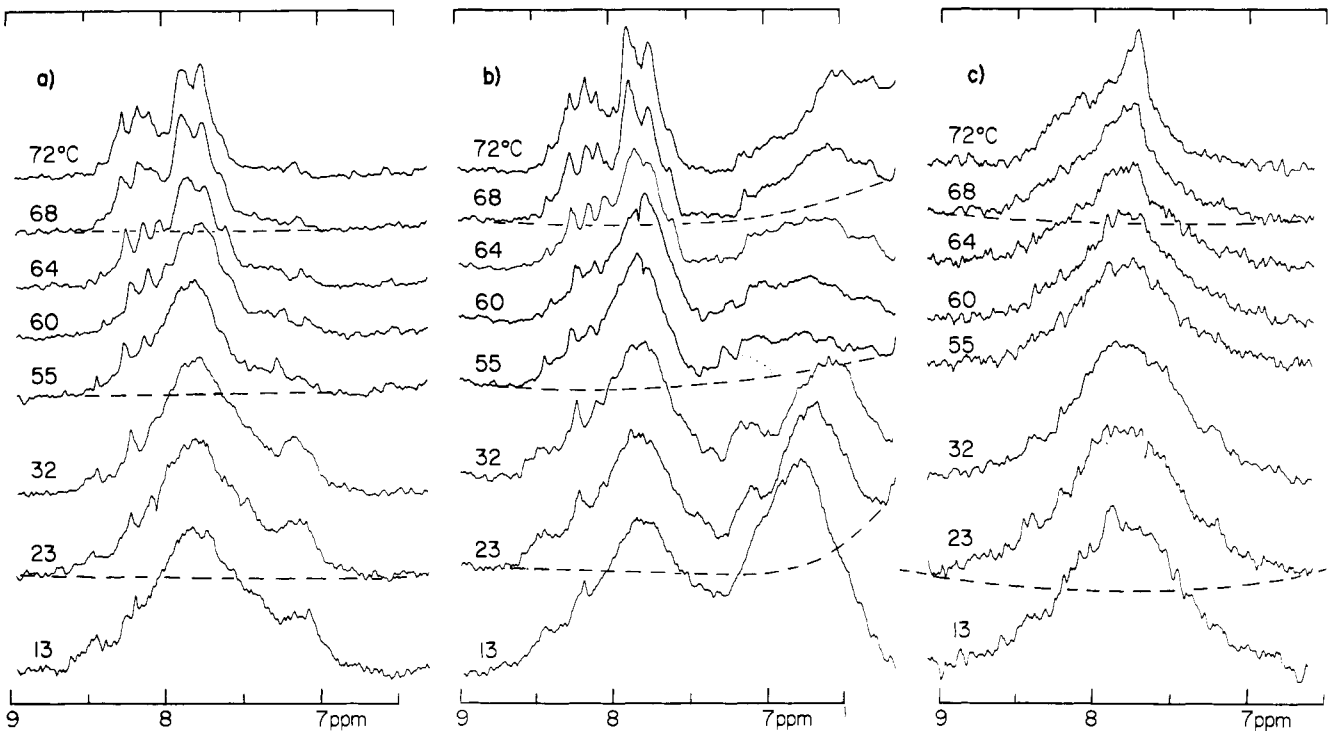

FIGURE 8: Temperature dependence of the aromatic spectrum of tRNA^{Tyr} (dimer) in D_2O (a) and in H_2O (b) under the same conditions as in Figure 9. The aromatic spectrum of unfractionated yeast tRNA (Plenum) (8.3 mg/ml) in D_2O (c) serves as an external intensity standard. All spectra were obtained under identical operating conditions and (a) and (b) may be directly compared.

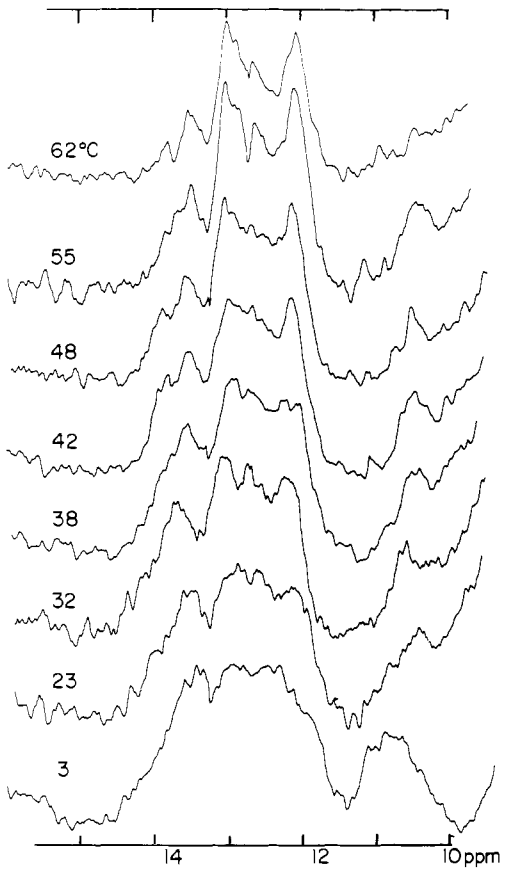

FIGURE 9: Temperature dependence of the low-field NMR spectrum of *E. coli* tRNA^{Tyr} (dimer) in 0.1 M NaCl, 10 mM cacodylic acid (pH 7.0), 1 mM EDTA, and 1 mM $Na_2S_2O_3$.

cently presented evidence that the majority of the Class I *E. coli* tRNA contains common tertiary structure base pairs that contribute resonances to the low-field spectrum at 14.8 ppm (assigned to A_{14}·s^4U_8), 13.8 ppm (assigned to A_{58}·T_{54}), 13.0 ppm (assigned to G_{19}·C_{56}), 11.5 ppm (assigned to U_{33}), and additional resonances at 10.5 and 9.5 ppm that have not been rigorously assigned (Bolton and Kearns, 1975; Kearns, 1976). It therefore seems reasonable to assign the "extra" resonances observed in the *E. coli* tRNA^{Tyr} spectrum at 13.8, 13.0, 11.5, and 10.5 ppm to the analogous tertiary interactions and this is consistent with the fact that these resonances melt out at relatively low temperatures (see Figure 4). What is surprising about the spectrum of the tRNA^{Tyr} monomer is the absence of a resonance at 14.8 ppm characteristic of the A_{14}·s^4U_8 tertiary structure base pair. The absence of this resonance cannot be attributed to dethiolation, since the optical measurements indicated the presence of two s^4U groups per molecule. Except for the lack of the resonance from A_{14}·s^4U_8, it would appear that most of the tertiary interactions common to other *E. coli* tRNA are also present in the tRNA^{Tyr} monomer.

Analysis of the Spectrum of Tyrosine Monomer in Low Salt. The spectrum of tyrosine tRNA monomer in low-salt solutions (1 mM $Na_2S_2O_3$), pH 7.0 (dialyzed), or 10 mM cacodylate buffer, pH 7.0 (added)) contains only 17 ± 2 resonances at 23 °C, and this represents a loss of about ten base pairs relative to the spectrum obtained in solutions containing higher salt or magnesium. As the analysis presented in Table II indicates, the differences can be accounted for in terms of loss of the three tertiary structure base pairs, three resonances from the minor stem, and three additional resonances from the hU stem. The 17 resonances that remain can be accounted for in terms of base pairs in the acceptor stem, the anticodon stem, and the TψC stem. The temperature dependence of the spectrum also supports this assignment (Figure 5). Between 23 and

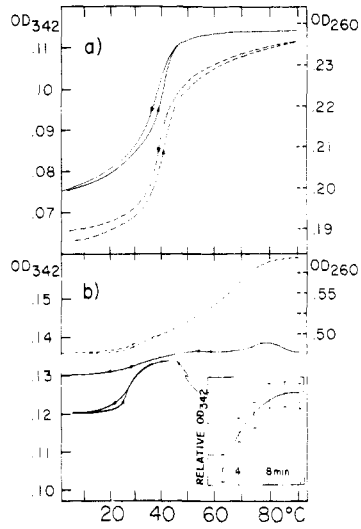

FIGURE 10: Optical melting curves of *E. coli* $tRNA^{Tyr}$ (monomer) under (a) low salt (10 mM cacodylic acid (pH 7.0), 1 mM EDTA, and 1 mM $Na_2S_2O_3$), and (b) high-salt conditions (same buffer plus 0.16 M NaCl). The s^4U absorption was monitored at 342 nm (–) (left scale); the 260-nm absorption is also shown (- - - -) (right scale). The sample could be reversibly heated and cooled in high salt to 36 °C (8 min above 30 °C); however, if it is heated to 44 °C rapid dimerization occurs (b insert).

45 °C there is a loss of approximately six resonances and the 45 °C spectrum can be well accounted for in terms of resonances from the anticodon stem and the acceptor stem. As discussed in the next section, the early melting of the hU, minor, and TψC stems is important to the interpretation of the dimerization phenomenon. The absence of a resonance from the fifth base pair at one terminus of the anticodon stem, A_{32}·ψ_{40} (45 °C), was expected on the basis of earlier studies of Aψ resonances at the terminus helices (Rordorf and Kearns, 1975; Wong and Kearns, 1974; Rordorf and Kearns, unpublished). The anomalous high-field position of the resonance from the neighboring G_{31}·C_{41} base pair may also be related to the early melting of the A_{32}·ψ_{40} base pair, to the possible base pairing isomerization of the pseudouridine, or to a specially pronounced ring current contribution from A_{32} under these special salt conditions.

Between 45 and 52 °C, four additional resonances are lost, and a good fit of the 52 °C spectrum is obtained if it is assumed that only the acceptor stem is still present (Table II).

Before closing this section we should point out that we cannot rigorously rule out the possibility that the monomer in low salt has an extended low-salt structure, such as the one proposed by Cole et al., 1972. The uncertainty is due to the possible early melting of the 19 base pairs of the low-salt structure proposed by Cole and the fact that a proportionately large number of terminal base pairs with uncertain resonance positions are present in this structure (acceptor stem, G_{66}·C_{12} to G_{62}·C_{16}, A_{22}·U_{56} to G_{24}·C_{54} and AC stem; Figure 1). The observation that the high-salt spectrum was obtained immediately after trapping the low-salt sample by the addition of magnesium to 10 mM (Figure 3b) does not necessarily rule out the presence of this structure, since spectra acquisition requires about 1 h. Finally, we should point out that the total sodium concentration (probably close to 0.1 M) is significantly higher with the tRNA concentrations used in the NMR experiments than in optical experiments under low-salt conditions and this may also explain the discrepancy between the optical melting point (Figure 10a) and the NMR melting under observed low-salt conditions (Figure 5).

Scheme I

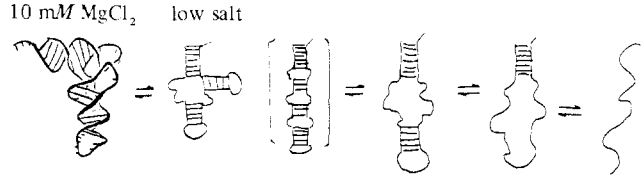

The sequence of melting of the monomer of *E. coli* $tRNA^{Tyr}$ under low-salt conditions can be summarized by Scheme I.

Model for the E. coli $tRNA^{Tyr}$ Dimer. In developing a model for the structure of the dimer, the following observations were taken into consideration. The NMR experiments indicate that dimerization involves the loss of approximately six base pairs per molecule, but that the dimer is relatively stable at elevated temperatures. The low-salt experiments demonstrated that the hU and minor stems melt early. Loss of these two stems along with some tertiary structure base pairs could then account for the reduced number of base pairs observed for the dimer, and at the same time permit formation of six new intermolecular base pairs in the dimer.

Optical melting studies, at 340 nm, also indicate that loss of tertiary structures is, by itself, not sufficient for dimer formation (Figure 10). The hypochromicity of the 4-thiouridine group is believed to monitor some tertiary structure features (Seno et al., 1969) and it is interesting to note that complete, although not instantaneous, reversibility was observed at 340 nm after heating a sample of $tRNA^{Tyr}$ monomers to 36 °C in relatively fast heating and cooling cycles (several minutes above 30 °C) (Figure 10b). A large irreversible hysteresis effect of the 335-nm absorption (monitored at 342 nm to eliminate 260 absorption) is, however, observed upon heating the same sample to 43 °C. This fairly rapid conversion to the dimer (monomer half-life in the order of minutes; Figure 10b insert) takes place at a temperature where the acceptor and anticodon stems, but not the TψC stem, were shown to be present in the low-field NMR spectrum of the monomer, even under lower salt conditions than used in the optical studies. This suggests that the TψC stem must be opened to form dimers.

On the basis of this information and a consideration of the base pairing matrix, we propose a dimer structure in which bases in the TψC stem and the TψC loop regions are involved in intermolecular base pairing (Figure 11). Topological considerations indicate that formation of this dimer does not require opening of the anticodon or acceptor stems, and this is in keeping with our observations on the monomer that indicate that these are the last two helices in the molecule to melt. Based on this model, the hysteresis observed on heating to 36 °C could be due to formation of an unstable dimer that involves intermolecular base pairing only between bases in the TψC loop and prevents immediate re-formation of the proper monomer structure.

The relatively elongated dimer structure that we propose contains a continuous 30 base-pair helix formed by stacking of the acceptor stems on the intermolecularly base paired TψC stems and the dimerized TψC loops. This special feature could account for the high stability of the dimer in spite of its relatively low number (20) of base pairs per tRNA (40/dimer).

Assignment of the Low-Field NMR Spectra of $tRNA^{Tyr}$ Dimer. Possible assignments of the low-field NMR spectrum (Figure 12b) based on this dimer structure (Figure 11) are given in Table II and a good fit between predicted and observed resonance positions can be seen for most of the resonances. The

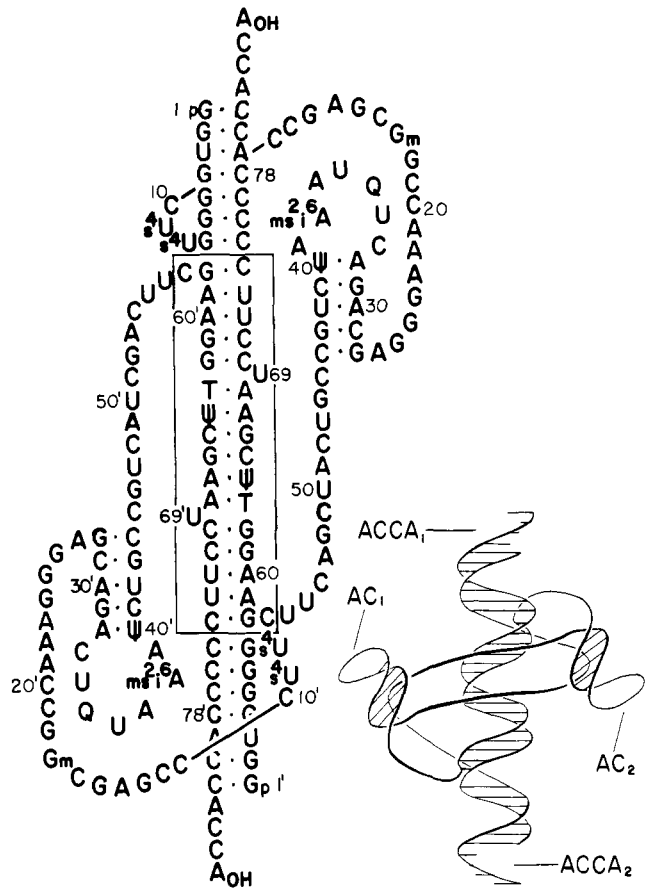

FIGURE 11: Proposed secondary (left) and tertiary (right) structure of the dimer of *E. coli* tRNA^{Tyr}. The intermolecular base pairs have been boxed in and the base numbers have been primed for one of the tRNA.

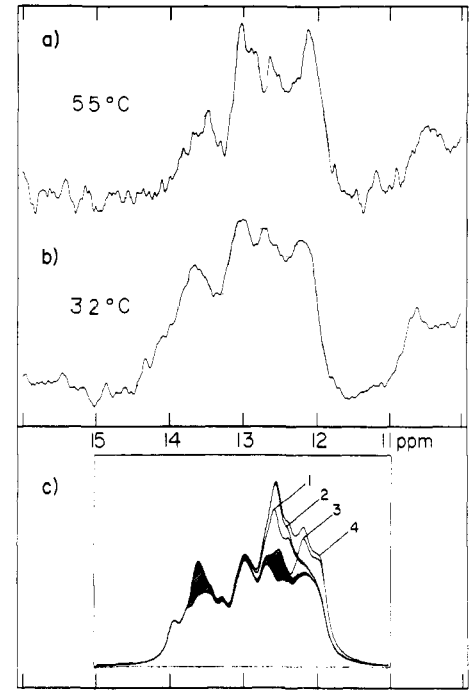

FIGURE 12: Comparison of the low-field NMR spectra (–) of *E. coli* tRNA^{Tyr} (dimer) (a) at 55 °C, (b) at 32 °C (from Figure 9) with the computer simulated spectra (·····) that contain 20 (a) and 19 (b) peaks of equal height and half-width (24 Hz = 0.08 ppm) at positions summarized in Table II. (c) Predicted low-field spectrum of the dimer (32 °C) supplemented by the complete base pairing of the minor stem (shaded areas) or by the base pairs of the hU stem (1), of the minor stem plus the hU stem (2), of the dimerized hU loop (G_{17}·C_{20}, 11.9 ppm; G_{18}·C_{19}, 12.15 ppm) (3), or of the dimer supplemented by all of these extra base pairs (4) whose resonances were placed at their positions observed in the monomer spectrum (Table II, 34 °C).

high-field positions of the resonances assigned to $\mathbf{G_7}$·C_{75} and $\mathbf{G_{58}}$·C_{74} are consistent with stacking of the acceptor stem on the intermolecular TψC stem and this stacking is an important feature of our proposed dimer model. The resonance from A_{68}·$\mathbf{T_{63}}$ appears to be absent at 32 °C, but this is not too surprising in view of its location adjacent to the abnormal uridine bulge, and indeed some spectral intensity is gained below 23 °C in the neighborhood of 14.3 ppm where it is predicted. The assigned position of G_{62}·C_{70} at somewhat lower fields than predicted may be another indication of this disturbance in the helical stacking.

Some extra spectral intensity below 13.5 ppm was assigned to the internal base pair A_{53}·$\mathbf{U_{47}}$ of the minor stem. The expected gain of intensity upon formation of the terminal GC base pairs of this short helix is indicated by the shaded areas in Figure 12c and these are indeed the regions where some additional intensity is observed in the low-temperature spectra (below 23 °C). A resonance around 13.8 ppm (tentatively assigned to the internal base pair A_{53}·$\mathbf{U_{47}}$ of the minor stem) melts out above 38 °C, and this loss, along with early melting of a resonance at ~13.0 (A_{32}·ψ_{40}?), leads to a total number of 18 resonances in the spectrum at 55 °C (Figures 9 and 12).

A Model for the Tertiary Structure of the Dimer of tRNA^{Tyr}. The question of why the, presumably less stable, minor stem helix might form instead of the hU stem (Figure 12c) may provide some clue as to the tertiary structure of the dimer. A study of a three-dimensional model of the proposed dimer structure (Figure 11) shows clearly that a long single strand from s^4U_8 to C_{57} is necessary. The *intra*molecular formation of the hU stem would remove 15 residues from the single strand, as compared to only 7 for the formation of the minor stem. Furthermore, the geometrical arrangement of the two single strands is such that an *inter*molecular base pairing of any of these helices *within* the dimer structure is impossible, but an intermolecular base pairing (involving bases of the hU stem and loop) between dimers to form polymers is likely. The presence of $2n$-mers and the absence of $2n + 1$-mers in our NMR sample was indeed confirmed by gel electrophoresis separation (Figure 7) and this explains the apparent loss of RNA concentration in the NMR spectra (aromatic region) upon dimerization of the NMR sample, which was partially regained in the NMR spectra at elevated temperatures.

The model of the dimer that we have proposed here includes some, but not all, features of a model proposed earlier by Yang et al. (1972). We, as they did, include intermolecular base pairing between the TψC loops; however, they also include *intermolecular* base pairing between bases in the minor and hU stems. As we have noted, this latter model leads to too many base pairs in the dimer and, as the analysis shown in Figure 12c indicates, the spectrum predicted for this particular dimer structure does not agree with the observed spectrum. Finally, formation of the Yang dimer requires opening and reclosing of the amino-acceptor stem helix. Since we find this to be the last structural feature to melt out, this seems unlikely.

The dimer structure that we have proposed is consistent with the thermodynamic, kinetic, optical, and NMR data, is topologically feasible, and accounts for formation of polymers with an even number of monomer units. Other plausible alternatives are seen to be inconsistent with our NMR observations.

Implications Regarding Dimerization of Other tRNA. The correlation between the self-complementarity of the TψC loop region (-TψCGAA- or -TψCGAG-) and the dimerization of various tRNAs was pointed out by Yang et al. (1972). The question of whether opening of the minor stem is required in the transition state of the dimer formation could be answered by the study of dimers of Class I or II tRNAs (short, non-base-paired minor stems) that also have self-complementary TψC loops. This group includes $tRNA^{Glu}_{II}$ and $tRNA^{Met}_{m}$ from *E. coli*, and $tRNA^{His}$ from salmonella. We have found that *E. coli* $tRNA^{Glu}_{II}$ (Class II) dimerizes (C. R. Jones, private communication) and that considerably larger amounts of tetramers than trimer are present in its higher aggregates (Rordorf, thesis). In the case of yeast $tRNA^{Leu}_{III}$ the formation of denatured monomer structure competes with the dimer formation (Adams et al., 1967; Kearns et al., 1974) but even then some dimer formation of this Class III tRNA has been observed (Kowalski and Fresco, 1971).

Acknowledgments

We acknowledge the contributions of Professor Brian R. Reid who participated in the initial study and provided samples of $tRNA^{Tyr}$ and Dr. Yeng P. Wong who carried out preliminary NMR studies of $tRNA^{Tyr}$. Recently, Professor Reid has independently carried out NMR studies of $tRNA^{Tyr}$ and developed an alternative model for the dimer structure. Mr. Philip Bolton kindly provided us with purified samples of *E. coli* $tRNA^{Tyr}_{I}$ and $tRNA^{Tyr}_{II}$.

References

Adams, A., Lindahl, T., and Fresco, J. R. (1967), *Proc. Natl. Acad. Sci. U.S.A. 57,* 1684–1691.

Bolton, P., and Kearns, D. R. (1975), *Nature (London) 255,* 347–349.

Bolton, P. H., Wong, K. L., Lerner, D., Jones, C., Kearns, D. R. (1976), *Biochemistry* (in press).

Cole, P. E., Yang, S. K., and Crothers, D. M. (1972), *Biochemistry 11,* 4358–4368.

Crothers, D. M., Hilbers, C. W., and Shulman, R. G. (1973), *Proc. Natl. Acad. Sci. U.S.A. 70,* 2899–2901.

Eisinger, J., and Gross, N. (1974), *J. Mol. Biol. 88,* 165–174.

Eisinger, J., and Spahr, P-F. (1973), *J. Mol. Biol. 73,* 131–137.

Erdmann, V. A., Sprinzl, M., and Pongs, O. (1973), *Biochem. Biophys. Res. Commun. 54,* 942–948.

Gillam, I., Millward, S., Blew, D., von Tigerstrom, M., Wimmer, E., and Tener, G. M. (1967), *Biochemistry 6,* 3043–3056.

Goodman, H. M., Abelson, J., Landy, A., Brenner, S., and Smith, J. D. (1968), *Nature (London) 217,* 1019–1024.

Grummt, F., Grummt, I., Gross, H. J., Sprinzl, M., Richter, D., and Erdmann, V. A. (1974), *FEBS Lett. 42,* 15–20.

Hawkins, E. R., and Chang, S. H. (1974), *Nucleic Acids Res. 1,* 1531–1538.

Högenaur, G. (1970), *Eur. J. Biochem. 12,* 527–532.

Kearns, D. R. (1976), *Prog. Nucleic Acid Res. Mol. Biol. 18* (in press).

Kearns, D. R., Jones, C. R., Wong, K. L., Wolfson, J. M. (1974), VIth International Conference on Magnetic Resonance in Biological Systems, Kandersteg, Switzerland, Abstract F.2.

Kearns, D. R., Patel, D. J., Shulman, R. G. (1971a), *Nature (London) 229,* 338–339.

Kearns, D. R., Patel, D., Shulman, R. G., and Yamane, T. (1971b), *J. Mol. Biol. 61,* 265–270.

Kearns, D. R., and Shulman, R. G. (1974), *Acc. Chem. Res. 7,* 33–39.

Kearns, D. R., and Wong, Y. P. (1974), *J. Mol. Biol. 87,* 755–774.

Kearns, D. R., Wong, Y. P., Chang, S. H., and Hawkins, E. (1974), *Biochemistry 13,* 4736–4746.

Kim, S. H., Suddath, F. L., Quigley, G. J., McPherson, A., Sussman, J. L., Wang, A. H. J., Seeman, N. C., and Rich, A. (1974), *Science 185,* 435–440.

Kowalski, S., and Fresco, J. R. (1971), *Science 172,* 384–385.

Lightfoot, D. R., Wong, K. L., Kearns, D. R., Reid, B. R., and Shulman, R. G. (1973), *J. Mol. Biol. 78,* 71–89.

Loehr, J. S., and Keller, E. B. (1968), *Proc. Natl. Acad. Sci. U.S.A. 61,* 1115–1122.

Nishimura, S., Harada, F., Narushima, U., and Seno, T. (1967), *Biochim. Biophys. Acta 142,* 133.

Pongs, O., Reinwald, E., and Stamp, K. (1971), *FEBS Lett. 16,* 275–277.

Richter, D., Erdmann, V. A., and Sprinzl, M., (1974), *Proc. Natl. Acad. Sci. U.S.A. 71,* 3226.

Robertus, J. D., Ladner, J. E., Finch, J. T., Rhodes, D., Brown, R. S., Clark, B. F. C., and Klug, A. (1974), *Nature (London) 250,* 546–551.

Rordorf, B. F., and Kearns, D. R. (1976a), *Biopolymers 15,* 325–336.

Rordorf, B. R., and Kearns, D. R. (1976b), *Anal. Biochem. 71,* 172–180.

Rordorf, B. F., Kearns, D. R., Hawkins, E., and Chang, S. H. (1976), *Biopolymers 15,* 325–336.

Schimmel, P. R., Uhlenbeck, O. C., Lewis, J. B., Dickson, L. A., Eldred, E. W., and Schrier, A. A. (1972), *Biochemistry 11,* 642–646.

Semancik, J. S., Morris, T. J., Weathers, L. G., Rordorf, B. F., and Kearns, D. R. (1975), *Virology 63,* 160–167.

Seno, T., Kobayashi, M., and Nishimura, S. (1969), *Biochim. Biophys. Acta 174,* 71–85.

Shulman, R. G., Hilbers, C. W., Wong, Y. P., Wong, K. L., Lightfoot, D. R., Reid, B. R., and Kearns, D. R. (1973), *Proc. Natl. Acad. Sci. U.S.A. 70,* 2042–2045.

Söll, D. G., Cherayil, J. D., and Bock, R. M. (1967), *J. Mol. Biol. 29,* 97–112.

Streeck, R. E., and Zachau, H. G. (1972), *Eur. J. Biochem. 30,* 382–391.

Uhlenbeck, O. C. (1972), *J. Mol. Biol. 65,* 25–41.

Williams, R. J. P. (1970) *Q. Rev., Chem. Soc. 24,* 331–365.

Wong, K. L., Bolton, P. H., and Kearns, D. R. (1975), *Biochim. Biophys. Acta 383,* 446–451.

Wong, K. L., and Kearns, D. R. (1974), *Biopolymers 13,* 371–380.

Wong, K. L., and Kearns, D. R. (1974), *Nature (London) 252,* 738–739.

Yang, S. K., Söll, D. G., and Crothers, D. M. (1972), *Biochemistry 12,* 2311–2320.

Zachau, H. G. (1968), *Eur. J. Biochem. 5,* 559–566.